

## Electron-phonon interaction in the normal and superconducting states of MgB<sub>2</sub>

Y. Kong, O. V. Dolgov, O. Jepsen, and O. K. Andersen  
*Max-Planck-Institut für Festkörperforschung, Stuttgart, Germany*  
 (Received 20 March 2001; published 30 May 2001)

For the 40 K superconductor MgB<sub>2</sub>, we have calculated the electronic and phononic structures and the electron-phonon (e-ph) interaction throughout the Brillouin zone *ab initio*. In contrast to the isoelectronic graphite, MgB<sub>2</sub> has holes in the bonding  $\sigma$  bands, which contribute 42% to the density of states:  $N(0) = 0.355$  states/(MgB<sub>2</sub>)(eV)(spin). The total interaction strength,  $\lambda = 0.87$  and  $\lambda_{tr} = 0.60$ , is dominated by the coupling of the  $\sigma$  holes to the bond-stretching optical phonons with wave numbers in a narrow range around  $590 \text{ cm}^{-1}$ . Like the holes, these phonons are quasi-two-dimensional and have wave vectors close to  $\Gamma A$ , where their symmetry is  $E$ . The  $\pi$  electrons contribute merely 0.25 to  $\lambda$  and to  $\lambda_{tr}$ . With Eliashberg theory we evaluate the normal-state resistivity, the density of states in the superconductor, and the B-isotope effect on  $T_c$  and  $\Delta_0$ , and find excellent agreement with experiments, when available.  $T_c = 40$  K is reproduced with  $\mu^* = 0.10$  and  $2\Delta_0/k_B T_c = 3.9$ . MgB<sub>2</sub> thus seems to be an intermediate-coupling e-ph pairing  $s$ -wave superconductor.

DOI: 10.1103/PhysRevB.64.020501

PACS number(s): 74.25.Kc, 63.20.Kr, 74.20.-z

The recent discovery<sup>1</sup> of superconductivity with  $T_c = 39$  K in the graphitelike compound MgB<sub>2</sub> has caused hectic activity. Density-functional (LDA) calculations<sup>2-5</sup> show that, in contrast to intercalated graphite ( $T_c \leq 5$  K) and alkali-doped fullerides, A<sub>3</sub>C<sub>60</sub> ( $T_c < 40$  K), in MgB<sub>2</sub> there are holes at the top of the B-B bonding  $\sigma$  bands, and that these couple rather strongly to optical B-B bond-stretching modes<sup>5</sup> with wave numbers<sup>2,4</sup> around  $600 \text{ cm}^{-1}$ . These are the same type of modes as those believed to couple most strongly to the  $\pi$  electrons in graphite and C<sub>60</sub>, where their wave numbers are 2.5 times larger, however.<sup>6,7</sup> Rough estimates<sup>2,5</sup> of the electron-phonon coupling strength for  $s$ -wave pairing in MgB<sub>2</sub> yield  $\lambda \sim 1$ . Measurements of the B-isotope effect<sup>8</sup> on  $T_c$ , tunnelling,<sup>9</sup> transport,<sup>10-13</sup> thermodynamic properties,<sup>10,14,15</sup> and the phonon density of states<sup>16,17</sup> confirm that MgB<sub>2</sub> is most likely an electron-phonon mediated  $s$ -wave superconductor with intermediate<sup>9,14,17</sup> or strong<sup>15</sup> coupling.

In order to advance, detailed comparisons between accurate results of Eliashberg theory and experiments are needed. Consider again the example of A<sub>3</sub>C<sub>60</sub>, also believed to be conventional  $s$ -wave superconductors<sup>7</sup> with  $T_c$ 's described by the McMillan expression:

$$T_c^{McM} = \frac{\omega_{ln}}{1.2} \exp \left[ \frac{-1.04(1+\lambda)}{\lambda - (1+0.62\lambda)\mu^*} \right]. \quad (1)$$

The LDA values for  $\lambda$  are 0.4–0.6 and the value of the Coulomb pseudopotential  $\mu^*$  to be used in Eq. (1) is presumably considerably larger than the usual value, 0.1–0.2, for  $sp$  materials<sup>18</sup> due to the small width ( $\sim 0.5$  eV) of the  $\pi t_{1u}$  subband compared with the on-ball Coulomb repulsion.<sup>7</sup> For MgB<sub>2</sub>, where the  $\pi$  band is 15 eV wide, one expects  $\mu^*$  to be 0.1–0.2 and the LDA (Ref. 19) plus generalized-gradient correction<sup>20</sup> to give  $\lambda$  with an accuracy better than 0.1. The result of such a  $\lambda$  calculation will be presented here and should allow us to reach conclusions about the superconductivity in MgB<sub>2</sub>.

MgB<sub>2</sub> consists of graphitelike B<sub>2</sub> layers stacked on top with Mg in between. The primitive translations are  $\mathbf{a} = (\sqrt{3}/2, 1/2, 0)a$ ,  $\mathbf{b} = (0, a, 0)$ ,  $\mathbf{c} = (0, 0, c)$ , with<sup>21</sup>  $a = 3.083 \text{ \AA} = 5.826 a_0$  and  $c/a = 1.142$ . In reciprocal space, and in units of  $2\pi/a$ , the primitive translations are:  $\mathbf{A} = (2/\sqrt{3}, 0, 0)$ ,  $\mathbf{B} = (-1/\sqrt{3}, 1, 0)$ ,  $\mathbf{C} = (0, 0, a/c)$ , and the points of high symmetry are:  $\Gamma = (0, 0, 0)$ ,  $\mathbf{A} = (0, 0, a/2c)$ ,  $\mathbf{M} = (1/\sqrt{3}, 0, 0)$ ,  $\mathbf{L} = (1/\sqrt{3}, 0, a/2c)$ ,  $\mathbf{K} = (1/\sqrt{3}, 1/3, 0)$ ,  $\mathbf{H} = (1/\sqrt{3}, 1/3, a/2c)$ . To reach a numerical accuracy exceeding 0.1 for  $\lambda$  requires careful sampling *throughout* the Brillouin zone for electrons as well as for phonons due to the small size of the cylindrical  $\sigma$ -hole sheets.<sup>2</sup> We therefore used Savrasov's<sup>18</sup> linear-response full-potential LMTO density-functional method, proven to describe the superconducting and transport properties of, e.g., Al and Pb with high accuracy. The Brillouin zone integrations were performed with the full-cell tetrahedron method<sup>22</sup> with the  $\mathbf{k}$ -points placed on the  $(\mathbf{A}, \mathbf{B}, \mathbf{C})/24$  sublattice. For the valence bands, a triple- $\kappa$   $spd$  LMTO basis set was employed and the Mg  $2p$ -semicore states were treated as valence states in a separate energy window. The charge densities and potentials were represented by spherical harmonics with  $l \leq 8$  inside the nonoverlapping MT spheres, and by plane waves with energies  $\leq 201$  Ry in the interstitial region.

The resulting electronic structure is practically identical to that of previous calculations.<sup>2-5</sup> Near and below the Fermi level there are two B  $p_z$   $\pi$  bands and three quasi-2D B-B bonding  $\sigma$  bands. The  $\sigma$  and  $\pi$  bands do not hybridize when  $k_z = 0$  and  $\pi/c$ . The  $\pi$  bands lie lower with respect to the  $\sigma$  bands than in graphite and have more  $k_z$  dispersion due to the influence of Mg, the on-top stacking, and the smaller  $c/a$  ratio. This causes the presence of  $p_{\sigma l} = 0.056$  light and  $p_{\sigma h} = 0.117$  heavy holes near the doubly degenerate top along  $\Gamma A$  of the  $\sigma$  bands. For the density of states at  $\varepsilon_F = 0$ , we find  $N(0) = N_{\sigma l}(0) + N_{\sigma h}(0) + N_{\pi}(0) = 0.048 + 0.102 + 0.205 = 0.355$  states/(MgB<sub>2</sub>) (eV) (spin).

The  $\sigma$  and  $\pi$  bands may be understood and described with reasonable accuracy near  $\varepsilon_F$  using the orthogonal tight-binding approximation with respect to the B  $p_z$  orbitals

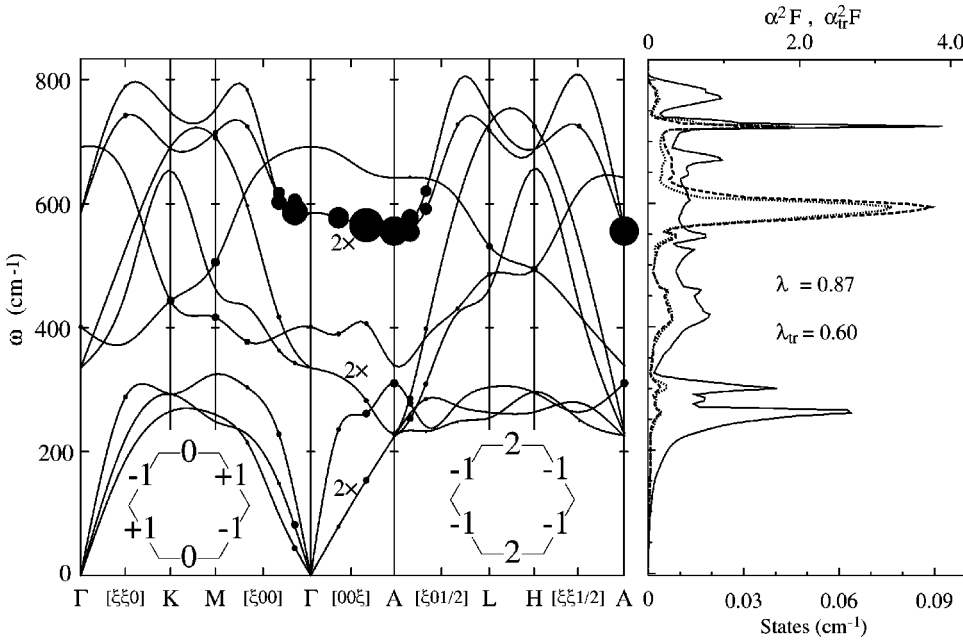


FIG. 1. Left: Calculated phonon dispersion curves in  $\text{MgB}_2$ . The area of each circle is proportional to the mode  $\lambda$ . The insets at the bottom show the two  $\Gamma A$   $E$  eigenvectors (not normalized), which apply to the holes at the top of the  $\sigma$  bands (bond-orbital coefficients) as well as to the optical bond-stretching phonons (relative change of bond lengths). Right:  $F(\omega)$  (full curve and bottom scale),  $\alpha^2(\omega)F(\omega)$  (broken), and  $\alpha_{tr}^2(\omega)F(\omega)$  (dotted). See text.

and the B-B two-center bond orbitals formed from the B  $sp^2$  hybrids: With two  $p_z$  orbitals per cell and hopping between nearest neighbors only ( $\varepsilon_z=0.04$  eV,  $t_z^\perp=0.92$  eV, and  $t_z=1.60$  eV), the  $\pi$  bands are  $\varepsilon_\pi(\mathbf{k})=\varepsilon_z+2t_z^\perp \cos ck_z \pm t_z \sqrt{1+4 \cos(ak_y/2)[\cos(ak_y/2)+\cos(ak_x\sqrt{3}/2)]}$ . The bonding  $\sigma$  band Hamiltonian is

$$H_\sigma(\mathbf{k})=t_{sp^2}-2t_b^\perp \cos ck_z-2t_b \begin{Bmatrix} 0 & \cos \gamma+r \cos(\alpha+\beta) & \cos \alpha+r \cos(\beta+\gamma) \\ \text{c.c.} & 0 & \cos \beta+r \cos(\alpha-\gamma) \\ \text{c.c.} & \text{c.c.} & 0 \end{Bmatrix},$$

in the representation of the three bond orbitals per cell, with  $t_{sp^2}$  being the energy of the two-center bond, and the integrals for hopping between nearest and second-nearest bond orbitals in the same layer being, respectively,  $t_b=5.69$  eV and  $t_b^\perp=rt_b=0.91$  eV, and with  $t_b^\perp=0.094$  eV being an order of magnitude smaller than  $t_b^\perp$ . Moreover,  $\alpha \equiv \frac{1}{2}\mathbf{k} \cdot \mathbf{a}$ ,  $\beta \equiv \frac{1}{2}\mathbf{k} \cdot \mathbf{b}$ , and  $\gamma \equiv \frac{1}{2}\mathbf{k} \cdot (\mathbf{b}-\mathbf{a})$ . Along  $\Gamma A$ ,  $\alpha=\beta=\gamma=0$  so that there is a singly degenerate band of symmetry  $A$  with dispersion  $t_{sp^2}-2t_b^\perp \cos ck_z-4(t_b+t_b^\perp)$ , and a doubly degenerate band of symmetry  $E$  with dispersion  $t_{sp^2}-2t_b^\perp \cos ck_z+2(t_b+t_b^\perp)$ . The  $E$  band is slightly above the Fermi level and its eigenvectors are given in the two inserts at the bottom of Fig. 1. The Fermi-surface sheets are warped cylinders<sup>2</sup> which may be described by expanding the two upper bands of  $H_\sigma(\mathbf{k})$  to lowest order in  $k_x^2+k_y^2 \equiv k_\parallel^2$ . This yields

$$\varepsilon_{\sigma n}(\mathbf{k})=\varepsilon_0-2t_b^\perp \cos ck_z-k_\parallel^2/m_{\sigma n}, \quad (2)$$

where  $\varepsilon_0 \equiv t_{sp^2}+2(t_b+t_b^\perp)=0.58$  eV is the average energy along  $\Gamma A$  and the units of  $k_\parallel^2/m_{\sigma n}$  and  $k_\parallel$  are, respectively, Ry and  $a_0^{-1}$ . The light and heavy-hole masses are, respectively,  $m_{\sigma l}=4/(t_b a^2)=0.28$  and  $m_{\sigma h}=4/(3t_b^\perp a^2)=0.59$ , relative to that of a free electron. For energies so closely below  $\varepsilon(\Gamma)$  that Eq. (2) holds, the number-of-states function is  $\int k_\parallel^2(\varepsilon, k_z) dk_z/k_{BZ}^2=k_\parallel^2(\varepsilon, \pi/2c)/k_{BZ}^2=(\varepsilon_0$

$-\varepsilon)m_{\sigma n}/k_{BZ}^2$ , and its energy derivative is therefore constant:  $N_{\sigma n}(\varepsilon)=m_{\sigma n}/k_{BZ}^2$ . Here,  $\pi k_{BZ}^2=(2\pi a_0/a)^2 2/\sqrt{3}$  is the area, and  $k_{BZ}$  the average radius of the Brillouin zone. Note that the  $\sigma$  sheets are quite narrow:  $k_{F\parallel l}(\pi/2c)/k_{BZ}=\sqrt{0.056/2}=0.17$  and  $k_{F\parallel h}(\pi/2c)/k_{BZ}=\sqrt{0.117/2}=0.24$ .

The dynamical matrix was calculated for  $\mathbf{q}$  points on the  $(\mathbf{A}, \mathbf{B}, \mathbf{C})/6$  sublattice using the B mass 10.811 which corresponds to the natural mix of isotopes. The phonon dispersions  $\omega_m(\mathbf{q})$  and density of states  $F(\omega)$  are shown in Fig. 1. The agreement between our  $F(\omega)$  and those obtained from inelastic neutron scattering<sup>16,17</sup> is excellent; our peaks at 260 and 730  $\text{cm}^{-1}$  (32 and 90 meV) are seen in the experiments at 32 and 88 meV. For the frequencies of the optical  $\Gamma$  modes we get 335  $\text{cm}^{-1}$  ( $E_{1u}$ ), 401  $\text{cm}^{-1}$  ( $A_{2u}$ ), 585  $\text{cm}^{-1}$  ( $E_{2g}$ ), and 692  $\text{cm}^{-1}$  ( $B_{1g}$ ). These values are in good agreement with those of previous calculations, except for the all-important  $E_{2g}$  modes where the LAPW (Ref. 2) and pseudopotential<sup>4</sup> calculations give values which are, respectively,  $\sim 100$   $\text{cm}^{-1}$  smaller and larger than ours. These doubly degenerate modes are the optical B-B bond-stretching modes (obs). Close to  $\Gamma A$ , they have exactly the same symmetry and similar dispersions as the light and heavy  $\sigma$  holes, although with the opposite signs. The  $E$  eigenfunctions shown at the bottom of Fig. 1 now refer to displacement patterns, e.g.,  $\{-1, 0, 1\}$  has one bond shortened, another

bond stretched by the same amount, and the third bond unchanged. These  $E$  displacement patterns will obviously modulate the electronic bond energy,  $t_{sp^2}$ , such as to split the light- and heavy-hole bands. An and Pickett<sup>5</sup> judged that the corresponding electron-phonon (e-ph) matrix element,  $g_{\sigma,obs}$ , will be the dominating one.

We now turn to the superconducting properties. Since the Fermi surface has two  $\sigma$  and two  $\pi$  sheets, one might expect anisotropic pairing with different gaps on different sheets. The experimental data,<sup>11,12</sup> however, demonstrate that a change of residual resistivity corresponding to a change of impurity scattering by two orders of magnitude hardly affects  $T_c$ , although  $T_c$  for anisotropic pairing is very sensitive to impurity scattering. We thus assume isotropic pairing. The relative linewidth of the  $m\mathbf{q}$  phonon due to e-ph coupling is<sup>23</sup>

$$\frac{\gamma_m(\mathbf{q})}{\omega_m(\mathbf{q})} = 2\pi \sum_{nn'\mathbf{k}} \delta[\varepsilon_n(\mathbf{k})] \delta[\varepsilon_{n'}(\mathbf{k}+\mathbf{q})] |g_{n\mathbf{k},n'\mathbf{k}+\mathbf{q},m}|^2 \\ \equiv \pi N(0) \omega_m(\mathbf{q}) \lambda_m(\mathbf{q}),$$

where the factor 2 is from spin degeneracy and  $\sum_{\mathbf{k}}$  is the average over the Brillouin zone, so that  $N(0) = \sum_{n\mathbf{k}} \delta[\varepsilon_n(\mathbf{k})]$ . We have (safely) assumed that  $\omega_m(\mathbf{q}) \ll \mathbf{q} \cdot \mathbf{v}_n(\mathbf{k})$ , where  $\mathbf{v}_n(\mathbf{k}) \equiv \nabla_{\mathbf{k}} \varepsilon_n(\mathbf{k})$  is the electron velocity. The e-ph matrix element is  $g_{n\mathbf{k},n'\mathbf{k}+\mathbf{q},m} = \langle n\mathbf{k} | \delta V | n'\mathbf{k} + \mathbf{q} \rangle / \delta Q_{m\mathbf{q}}$ , where the displacement in the  $i$  direction of the  $j$ th atom is related to the phonon eigenvector  $e_{ij,m\mathbf{q}}$  and displacement  $\delta Q_{m\mathbf{q}}$  by  $\delta R_{ij} = e_{ij,m\mathbf{q}} \delta Q_{m\mathbf{q}} / \sqrt{2M_j \omega_{m\mathbf{q}}}$ . The Eliashberg spectral function is

$$\alpha^2(\omega) F(\omega) \equiv \frac{1}{2\pi N(0)} \sum_{m\mathbf{q}} \frac{\gamma_m(\mathbf{q})}{\omega_m(\mathbf{q})} \delta[\omega - \omega_m(\mathbf{q})],$$

and the strength of the e-ph interaction is finally  $\lambda \equiv 2 \int_0^\infty \omega^{-1} \alpha^2(\omega) F(\omega) d\omega = \sum_{m\mathbf{q}} \lambda_m(\mathbf{q})$ .

The dominance of the  $\sigma$ - $\sigma$  coupling via the optical bond-stretching mode is clearly seen in Fig. 1, where the area of a black circle is proportional to  $\lambda_m(\mathbf{q})$ . Along  $\Gamma A$ , except when  $\mathbf{q} \cdot \mathbf{v} < \omega$ , only the small  $k_z$  dispersion ( $t_b^+$ ) makes  $\lambda_m(\mathbf{q})$  not diverge so that the numerical values are inaccurate due to the relative coarseness of our  $\mathbf{k}$  mesh. The nearly cylindrical  $\sigma$  sheets, whose diameters are of about the same size as the smallest, nonzero  $q_{\parallel}$  on the affordable  $(\mathbf{A}, \mathbf{B}, \mathbf{C})/6$  mesh, require even more care in the numerical  $\mathbf{q}$  integration: In the case of a single cylindrical sheet with  $p$  holes,  $\lambda(q_{\parallel})$  has the well-known  $\text{Im}\chi(q_{\parallel}, \omega \rightarrow 0)$  form:  $\lambda(q_{\parallel})/\lambda = (2\pi p x \sqrt{1-x^2})^{-1} \theta(1-x)$  with  $x = q_{\parallel}/2k_{F\parallel}$ . This function vanishes when  $q_{\parallel} > 2k_{F\parallel}$ , has a flat minimum of value  $(\pi p)^{-1}$  near  $q_{\parallel} = \sqrt{2}k_{F\parallel}$ , and has integrable divergencies at  $q_{\parallel} = 2k_{F\parallel}$  and 0. The proper average of  $\lambda(q_{\parallel})$  is  $\lambda$ . This means that  $\lambda(\mathbf{q})$  calculated on a coarse mesh scatter violently for small  $|\mathbf{q}|$ , but that weighting with  $\lambda/\lambda(q_{\parallel})$  gives the same correct result for all these points, provided that warping, as well as  $\mathbf{k}, \mathbf{k}'$  dependence of  $g$  and  $\omega$ , are neglected. In the case of two cylindrical sheets, and no coupling between them,  $\lambda_n(q_{\parallel})/\lambda_n$  should be weighted by  $m_n^2/(m_1^2 + m_2^2)$ . In our numerical evaluation of the e-ph interaction with the linear-response code<sup>18</sup> we discarded the val-

ues of  $\lambda_m(\mathbf{q})$  with  $\mathbf{q}$  along  $\Gamma A$ , and added those on the  $(\mathbf{A}/12, \mathbf{B}/12, \mathbf{C}/6)$  mesh for which  $\sqrt{2}k_{F\parallel} \lesssim q_{\parallel} \lesssim \sqrt{2}k_{F\parallel h}$ . The result was  $\lambda = 0.62 + 0.25$ , where 0.62 was the contribution from  $\mathbf{q}$ 's so small that  $\sigma$ - $\sigma$  coupling occurs, and 0.25 was the contribution from the remaining part of  $\mathbf{q}$  space, which must involve a  $\pi$  sheet. Had we included the inaccurate  $\lambda_m(\mathbf{q})$  values along the  $\Gamma A$  line, the  $\sigma$ - $\sigma$  result would have been 0.72 instead of 0.62. The result was finally checked by using the approximate  $\lambda(q_{\parallel})/\lambda$  correction for the point  $\mathbf{q} = \mathbf{A}/12$ . This yielded 0.58 instead of 0.62. In conclusion:  $\lambda = 0.87 \pm 0.05 = (0.62 \pm 0.05) + 0.25 \equiv \lambda_{\sigma} + \lambda_{\pi}$ . This value is larger than the rigid-atomic-sphere estimate of Kortus *et al.*<sup>2</sup> ( $\lambda \approx 0.7$ ) and smaller than the estimate of An and Pickett<sup>5</sup> ( $\lambda \approx 0.95$ ), who assumed pairing for the  $\sigma$  sheets only (anisotropic pairing).

The Eliashberg function shown on the right-hand side of Fig. 1 is dominated by the large  $\sigma$ - $\sigma$  peak around  $\omega_{obs} = 590 \text{ cm}^{-1} = 73 \text{ meV}$ . The fact that the  $\sigma$  sheets are narrow, warped cylinders whose coupling is dominated by the optical bond-stretching mode, and that the coupling between  $\sigma$  and  $\pi$  sheets is negligible, lead to the following approximation:

$$\alpha^2(\omega) F(\omega) \approx \alpha_{\pi}^2(\omega) F(\omega) [N_{\pi}(0)/N(0)] \\ + |g_{\sigma,obs}|^2 \delta(\omega - \omega_{obs}) N_{\sigma}^2(0)/N(0),$$

where  $\alpha_{\pi}^2(\omega) F(\omega)$  is the usual expression, but with  $\pi$  electrons only.

Knowing  $\alpha^2(\omega) F(\omega)$  and a value of the Coulomb pseudopotential  $\mu^*(\omega_c)$ , we solve the Eliashberg equation on the real frequency axis,<sup>24</sup> and obtain  $T_c = 40 \text{ K}$  if  $\mu^*(\omega_c) = 0.14$ . Taking retardation effects into account, we find  $\mu^* \equiv \mu^*(\omega_c) / [1 + \mu^*(\omega_c) \ln(\omega_c/\omega_{ln})] = 0.10$ , where  $\omega_{ln} = 504 \text{ cm}^{-1} = 62 \text{ meV}$  is obtained from  $0 = \int_0^\infty \ln(\omega/\omega_{ln}) \omega^{-1} \alpha^2(\omega) F(\omega) d\omega$ , and the cut-off frequency is taken as  $\omega_c = 10 \max \omega = 8000 \text{ cm}^{-1}$ . This value of  $\mu^*$  is at the lower end of what is found for simple  $sp$  metals.<sup>18</sup> The relation back to a screened Coulomb interaction  $U$  is  $\mu^* = \mu / [1 + \mu \ln(\omega_p/\omega_{ln})]$ , where  $\mu = UN(0)$  and  $\omega_p \sim 7 \text{ eV}$  is the plasma frequency given below. We thus find  $\mu = 0.19$  and  $U = 1.1 \text{ eV}$ , which are normal values. Had we used the approximate McMillan expression (1), the slightly higher value  $\mu^* = 0.14$  would be needed to reproduce the experimental  $T_c$ .

In Fig. 2 we show our Eliashberg calculation with  $\mu^* = 0.10$  of the square of the density of states,  $N_s(\varepsilon)/N(0) = \text{Re} [\varepsilon / \sqrt{\varepsilon^2 - \Delta_{3K}^2(\varepsilon)}]$ , in the superconductor. The BCS singularity is at  $\varepsilon = \Delta_{3K}(0) = 6.8 \text{ meV}$ , which is in accord with the 4.9–6.9 meV found in tunneling experiments.<sup>9</sup> This yields  $2\Delta_0/k_B T_c = 3.9$  which is slightly higher than the BCS value of 3.52. The distinct feature near 80 meV corresponds to the peak in  $\alpha^2(\omega) F(\omega)$  at 73 meV, shifted by the 6.8 meV gap. The latter function is also shown in the figure together with the measurable quantity  $-d^2 I/dV^2 \sim -dN_s(\varepsilon)/d\varepsilon$ .

We have calculated the change in  $T_c$  upon isotope substitution of  $^{11}\text{B}$  for  $^{10}\text{B}$  and get  $\delta T_c = -1.7 \text{ K}$ , which corresponds to the exponent  $-\delta \ln T_c / \delta \ln M_B = 0.46$ . This agrees

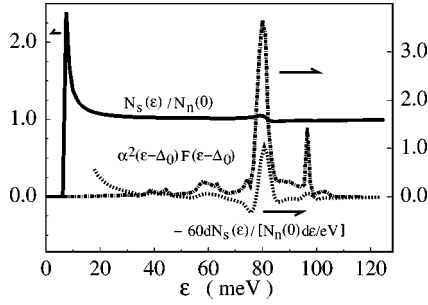


FIG. 2. Normalized density of states (full) and the negative of its energy derivative (dotted) as obtained from the Eliashberg equation with  $\mu^* = 0.10$  and  $T = 3$  K.

well with the measured<sup>8</sup> value  $\delta T_c = -1$  K. For the change of the gap, which may be measured in tunnelling and optical experiments, we calculate  $\delta \Delta_0 = -1.9$  cm<sup>-1</sup>, which corresponds to the exponent  $-\delta \ln \Delta_0 / \delta \ln M_B = 0.38$ .

Finally, we have considered transport properties in the normal state. Here, the solution of the kinetic equation leads to the transport e-ph spectral function  $\alpha_{tr,x}^2(\omega)F(\omega)$ , and similarly for  $y$  and  $z$ . These components are given by the previous expressions, but with the additional factor  $[v_{nx}^2(\mathbf{k}) - v_{nx}(\mathbf{k})v_{n'x}(\mathbf{k} + \mathbf{q})] / \langle v_x^2 \rangle$  inserted.  $\langle v_x^2 \rangle \equiv N(0)^{-1} \sum_{n\mathbf{k}} v_{nx}^2(\mathbf{k}) \delta[\epsilon_n(\mathbf{k})]$ . In Fig. 1 the directional average,  $\alpha_{tr}^2(\omega)F(\omega)$ , is seen to have the same shape as  $\alpha^2(\omega)F(\omega)$ , except for the  $\sigma$ - $\sigma$  interaction via the optical bond-stretching modes, whose  $\alpha_{tr}^2(\omega)F(\omega)$  is smaller, presumably due to the near two-dimensionality of the  $\sigma$  bands. As a result,  $\lambda_{tr} = 0.60$ . For the plasma frequencies,  $\omega_{p,x}^2 = 4\pi e^2 N(0) \langle v_x^2 \rangle / [\mathbf{abc}]$ , we find  $\omega_{p,x} = \omega_{p,y} = 7.02$  eV and  $\omega_{p,z} = 6.68$  eV. Also, the temperature dependence of the specific dc resistivity calculated with the standard Bloch-Grüneisen expression,  $\rho_{dc,x}(T) = (\pi/\omega_{p,x}^2 T) \int_0^\infty \omega \sinh^{-2}(\omega/2T) \alpha_{tr,x}^2(\omega)F(\omega) d\omega$ , is nearly isotropic and, as shown in Fig. 3, is in accord with recent measurements on dense wires<sup>12</sup> over the entire temperature

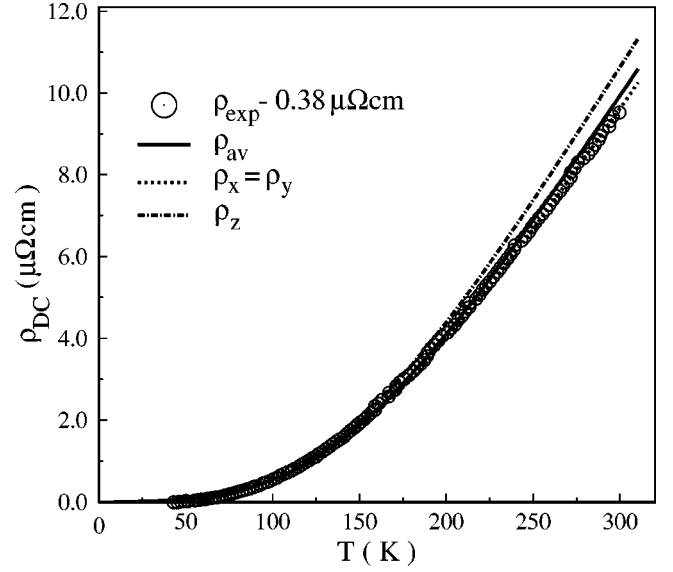


FIG. 3. Calculated dc resistivities in different directions compared with the experiment in Ref. 12.

range. The crossover from power law to linear temperature dependence is seen to occur near  $\max \omega/5 = 160$  cm<sup>-1</sup> = 230 K, as expected.<sup>25</sup>

In conclusion, we have presented an accurate *ab initio* calculation of the e-ph interaction in MgB<sub>2</sub> and find  $\lambda = 0.87 \pm 0.05$ . Eliashberg theory with  $\mu^* = 0.10$  gives good agreement with available experiments and several predictions. The unexpected high  $T_c$  is due to the large  $\lambda$  value caused by the presence of holes in the B-B bonding  $\sigma$  band and the relative softness of the optical bond-stretching modes. MgB<sub>2</sub> thus seems to be a simple and clear case of an intermediate-coupling e-ph pairing *s*-wave superconductor.

Useful discussions with R. K. Kremer, I. I. Mazin, W. E. Pickett, S. Savrasov, D. Savrasov, and S. V. Shulga are acknowledged.

<sup>1</sup>J. Nagamatsu *et al.*, Nature (London) **410**, 63 (2001).

<sup>2</sup>J. Kortus *et al.*, Phys. Rev. Lett. **86**, 4656 (2001).

<sup>3</sup>K.D. Belashchenko *et al.*, cond-mat/0102290 (unpublished).

<sup>4</sup>G. Satta *et al.*, cond-mat/0102358 (unpublished).

<sup>5</sup>J.M. An and W.E. Pickett, Phys. Rev. Lett. **86**, 4366 (2001).

<sup>6</sup>C.T. Chan *et al.*, Phys. Rev. B **36**, 3499 (1987).

<sup>7</sup>O. Gunnarsson, Rev. Mod. Phys. **69**, 575 (1997).

<sup>8</sup>S.L. Bud'ko *et al.*, Phys. Rev. Lett. **86**, 1877 (2001).

<sup>9</sup>A. Sharoni *et al.*, cond-mat/0102325, Phys. Rev. B (to be published 1 June 2001).

<sup>10</sup>D.K. Finnemore *et al.*, Phys. Rev. Lett. **86**, 2420 (2001).

<sup>11</sup>C.U. Jung *et al.*, cond-mat/0102215 (unpublished).

<sup>12</sup>P.C. Canfield *et al.*, Phys. Rev. Lett. **86**, 2423 (2001).

<sup>13</sup>S.L. Bud'ko, *et al.*, Phys. Rev. B **63**, 220503 (2001).

<sup>14</sup>R.K. Kremer *et al.*, cond-mat/0102432 (unpublished).

<sup>15</sup>Ch. Wälti *et al.*, cond-mat/0102522 (unpublished).

<sup>16</sup>T.J. Sato *et al.*, cond-mat/0102468 (unpublished).

<sup>17</sup>R. Osborn *et al.*, cond-mat/0103064 (unpublished).

<sup>18</sup>S.Y. Savrasov, Phys. Rev. B **54**, 16 470 (1996); S.Y. Savrasov and D.Y. Savrasov, *ibid.* **54**, 16 487 (1996).

<sup>19</sup>S.H. Vosko *et al.*, Can. J. Phys. **58**, 1200 (1980).

<sup>20</sup>J.P. Perdew *et al.*, Phys. Rev. Lett. **77**, 3865 (1996).

<sup>21</sup>A. Lipp and M. Roder, Z. Anorg. Chem. **334**, 225 (1966).

<sup>22</sup>P.E. Blöchl *et al.*, Phys. Rev. B **49**, 16 223 (1994).

<sup>23</sup>P.B. Allen and B. Mitrović, Solid State Phys. **37**, 1 (1982).

<sup>24</sup>S.V. Shulga (unpublished).

<sup>25</sup>P.B. Allen *et al.*, Phys. Rev. B **34**, 4331 (1986).